Draft version February 2, 2008
Preprint typeset using LaTeX style emulateapj v. 11/12/01

THE DEUTERIUM-TO-OXYGEN RATIO IN THE INTERSTELLAR MEDIUM

Guillaume Hébrard[1]
Institut d'Astrophysique de Paris, CNRS, 98^{bis} boulevard Arago, F-75014 Paris, France

and

H. Warren Moos
Department of Physics and Astronomy, Johns Hopkins University, Baltimore, MD 21218, USA

Draft version February 2, 2008

ABSTRACT

Because the ionization balances for H I, O I, and D I are locked together by charge exchange, the deuterium-to-oxygen ratio, D/O, is an important tracer for the value of the D/H ratio and for potential spatial variations in the ratio. As the D I and O I column densities are of similar orders of magnitude for a given sight line, comparisons of the two values will generally be less subject to systematic errors than comparisons of D I and H I, which differ by about five orders of magnitude. Moreover, D/O is additionally sensitive to astration, because as stars destroy deuterium, they should produce oxygen. We report here the results of a survey of D/O in the interstellar medium performed with the Far Ultraviolet Spectroscopic Explorer (*FUSE*). We also compare these results with those for D/N. Together with a few results from previous missions, the sample totals 24 lines of sight. The distances range from a few pc to ~ 2000 pc and $\log N(\mathrm{D\ I})$ from ~ 13 to ~ 16 (cm^{-2}). The D/O ratio is constant in the local interstellar medium out to distances of ~ 150 pc and $N(\mathrm{D\ I}) \simeq 1 \times 10^{15}\,\mathrm{cm}^{-2}$, *i.e.* within the Local Bubble. In this region of the interstellar space, we find $\mathrm{D/O} = (3.84 \pm 0.16) \times 10^{-2}$ ($1\,\sigma$ in the mean). The homogeneity of the local D/O measurements shows that the spatial variations in the local D/H and O/H must be extremely small, if any. A comparison of the Local Bubble mean value with the few D/O measurements available for low metallicity quasar sight lines shows that the D/O ratio decreases with cosmic evolution, as expected. Beyond the Local Bubble we detected significant spatial variations in the value of D/O. This likely implies a variation in D/H, as O/H is known to not vary significantly over the distances covered in this study. Our dataset suggests a present-epoch deuterium abundance below 1×10^{-5}, *i.e.* lower than the value usually assumed, around 1.5×10^{-5}.

Subject headings: ISM: abundances – ISM: clouds – cosmology: observations – ultraviolet: ISM – (stars:) white dwarfs– (stars:) subdwarfs

1. INTRODUCTION

It is generally believed that deuterium was produced in significant amounts only during the primordial nucleosynthesis of the Big Bang (BBN). Since then, deuterium has been steadily destroyed in stellar interiors by nuclear processes. Thus, its abundance compared to hydrogen, D/H, is a key measurement for studies of both cosmology and galactic chemical evolution (see, *e.g.*, Vangioni-Flam et al. 2000). Although the evolution of the deuterium abundance seems to be qualitatively understood, important questions remain open.

In this paper we focus on the abundance of deuterium in the interstellar medium (ISM), which is characteristic of the present-day Galactic deuterium abundance. $(\mathrm{D/H})_{\mathrm{ISM}}$ measurements prior to the Far Ultraviolet Spectroscopic Explorer (*FUSE*) mission showed some dispersion (see, *e.g.*, Lemoine et al. 1999 for a review). This dispersion likely results from poorly understood physical processes (*e.g.* astration and transport), although the effects of unidentified systematic errors cannot be completely ruled out. There has been considerable debate of these issues and final resolution will have implications for our understanding of the physics of the interstellar medium, the chemical evolution of the Galaxy, and the baryonic density of the Universe inferred from primordial D/H measurements (see also Moos et al. 2002; Hoopes et al. 2003).

An accurate determination of interstellar deuterium abundances is one of the main objectives of the *FUSE* mission, which was launched in 1999 (Moos et al. 2000). The *FUSE* bandpass ranges from 905 Å to 1187 Å, so it includes all the D I transitions of the Lyman series except for Ly-α. We report here the first results of a survey of D/O in the ISM. This survey includes already published *FUSE* results, together with additional new *FUSE* results obtained toward seven targets. The first *FUSE* measurements of D/O were presented by Moos et al. (2002) and references therein. This earlier study was based on only seven targets and a good understanding of the D/O ratio was limited by low number statistics. Additional measurements by other authors and the new ones reported here increase the number of *FUSE* sight lines to 19. Together with five measurements from previous missions, the present study includes abundance measurements toward 24 lines of sight in the Galactic disk. The sample includes a wide variety of sight lines; the deuterium column densities vary over three orders of magnitude and the sight line distances range from within the Local Bubble to ~ 2000 pc.

The measured deuterium abundance by number is usu-

[1] email: hebrard@iap.fr

ally compared to that of hydrogen. One of the challenges of D/H measurements is to evaluate two measurements for the same line of sight, namely the H I and D I column densities, which differ by about five orders of magnitude. Such a large difference is a potential source of systematic errors. For example, all lines from the same species may lie on the non-linear part of the curve of growth, or there may be clouds in which H I column densities are detectable, but whose D I column densities are below the detection limit (see, *e.g.*, Linsky & Wood 1996, Lemoine et al. 2002, or Vidal-Madjar & Ferlet 2002).

Many of the difficulties associated with obtaining accurate D/H measurements may be avoided by measuring the deuterium-to-oxygen ratio, D/O (see, *e.g.*, Timmes et al. 1997). First of all, as discussed above, the D/O ratio is of order of a few percent rather than $\sim 10^{-5}$ as for the case of D/H, thus the D I and O I column density measurements are not subject to some of the systematic errors associated with measurements of D/H. In addition to the D I transitions, many O I transitions with different oscillator strengths are present in the *FUSE* bandpass, allowing measurement of the O I and the D I column densities over a wide range of values. O I is believed to be a good tracer of H I in the nearby Galactic disk (Meyer et al. 1998; André et al. 2003). The neutral forms of oxygen and hydrogen likely dominate over their ions for many sight lines in the diffuse interstellar medium. In any case, because both species have nearly the same ionization potentials, their ionization balances for the two species are strongly coupled to each other by charge exchange reactions (Jenkins et al. 2000). Thus, no corrections from ionization models are required, and we will use D/O for N(D I)/N(O I) hereafter. Finally, D/O is very sensitive to stellar activity, because of both deuterium destruction (deuterium is burned in stellar atmospheres at temperatures as low as 6×10^6 K) and oxygen production (oxygen is mainly produced by type II supernovae). Hence, spatial variations of the deuterium abundance due to different astration rates in different locations would cause even higher D/O spatial variations. We use a D/O point of view in the present paper, consciously avoiding a reliance on H I column density measurements. We also compare D/O *vs.* D/N, since nitrogen is often assumed to be also a good hydrogen tracer (Ferlet 1981; Meyer et al. 1997).

The new *FUSE* data and their processing are presented in Sect. 2, and the method of analysis in Sect. 3. The individual targets for which we present new *FUSE* column density measurements here are discussed in Sect. 4. The first results of the survey are reported in Sect. 5 and discussed in Sect. 6.

2. OBSERVATIONS AND DATA PROCESSING

The new *FUSE* data presented here were obtained in 2000, 2001, and 2002 as part of Science Team D/H programs, calibration programs, and a Guest Investigator program. The log of the observations is reported in Table 1. They were obtained in histogram or time-tagged modes, through the low (LWRS), medium (MDRS), or high (HIRS) resolution slit. Details of the *FUSE* instrument may be found in Moos et al. (2000) and Sahnow et al. (2000).

The one-dimensional spectra were extracted from the two-dimensional detector images and calibrated using the CalFUSE pipeline. We used the most recent version of CalFUSE available at the time of the extraction. The different improvements of CalFUSE include, among others, corrections of event bursts, thermal drift, geometric distortions, or astigmatism. No significant effects on column density measurements were found between these different versions. In particular, no effects on the zero flux level were found. Each *FUSE* observation is split up into individual exposures. They were co-added separately for each channel (SiC1, SiC2, LiF1, and LiF2) and for a given slit, after correcting for relative wavelength offsets between individual calibrated exposures (typically, a few *FUSE* pixels). This correction procedure improved the spectral resolution slightly and helped average out fixed pattern noise in the detector, acting as a random FP-Split procedure (Kruk et al. 2002). Exposures with strong airglow emissions or unacceptably low signal-to-noise ratios were not included in the final sums.

All of the spectra were binned to three *FUSE* pixels. The resolving power in the final spectra ranges between $\sim$ 13000 and $\sim$ 18500 (full width at half maximum, *i.e.* around 10 *FUSE* pixels), depending on channel and wavelength, and on the slit used. These values are similar to those found previously on *FUSE* data obtained toward similar point-like sources and extracted with versions 1.7 or 1.6 of CalFUSE (Hébrard et al. 2002; Wood et al. 2002a).

3. DATA ANALYSIS

Column density measurements were obtained by profile fitting of the interstellar spectral absorption lines obtained towards the lines of sight studied. We focus here on results for the D I, O I, and N I column densities, in order to compare D/O and D/N results. We used the profile fitting method presented in detail by Hébrard et al. (2002). It is briefly described below.

Spectral windows (see examples in Figures 1-3) including D I, O I, N I, and other species transitions were extracted from the *FUSE* spectra available for each of the different datasets (Table 1) and fitted simultaneously with the Owens.f procedure. This software, which has been developed by Martin Lemoine and the French *FUSE* Team, finds the best Voigt profiles compatible with all the spectral windows, using χ^2 minimization. Several parameters are free to vary during the fitting procedure, including the column densities, the radial velocities of the interstellar clouds, their temperatures and turbulent velocities, and the shapes of the stellar continua, which are modeled by low order polynomials.

Some instrumental parameters are also free to vary, including the spectral shifts between the different spectral windows (in order to correct for inaccuracies of the *FUSE* wavelength calibration) and the widths of the Gaussian Line Spread Functions (LSF) used to convolve with the Voigt profiles (the *FUSE* LSF is not determined accurately, but it probably depends on the channel and the wavelength). The fits include only unsaturated lines in order to reduce uncertainties resulting from saturation effects and other systematic errors. The plots of the fits prior to convolution with the LSF give us the saturation criterion, following the method used by Hébrard et al. (2002):

all the lines with un-convolved absorption profiles reaching close to the zero flux level were not included in the final fits. As D I, O I, and N I transitions are numerous in the *FUSE* bandpass, with a large range of oscillator strengths, it was possible to fit numerous unsaturated lines for most of the targets (see Table 2).

The laboratory wavelengths and oscillator strengths are from Morton (1991; 2003). When needed, those of H_2 were added from a compilation by E. Roueff (Abgrall et al. 1993a, 1993b). For the lines that we used, no biases due to oscillator strength uncertainties were found (see tests on oscillator strength values in Hébrard et al. 2002). Only one interstellar component was assumed for each target. This assumption is unlikely to be true for many lines of sight, but it will have no effect on the column densities measured from unsaturated lines (see tests of this assumption in Hébrard et al. 2002). Thus, we report total column densities, integrated along each line of sight.

The simultaneous fitting of numerous unsaturated lines allow statistical and systematic errors to be reduced, especially those due to continuum placements, LSF uncertainties, line blending, flux and wavelength calibrations, and atomic data uncertainties. The 1-σ error bars were computed using the $\Delta\chi^2$ method; both statistical and systematic effects were taken into account. The details of the $\Delta\chi^2$ method may be found in Hébrard et al. (2002).

The D I, O I, and N I lines included in the fits are reported in Table 2. Note that due to the redundancy of the *FUSE* wavelength coverage (and to the use of several slits for some targets), a given transition may be observed several times. These independent observations are all included in the fits, allowing the reduction of the error bars, and identification of possible instrumental artifacts.

4. INDIVIDUAL TARGETS

We discuss here the seven individual targets with new *FUSE* results.

4.1. *Sirius B*

D I and N I interstellar column densities were measured from HST-GHRS spectra by Hébrard et al. (1999) for the two interstellar components detected along the line of sight to the white dwarf Sirius B. Using these results, we adopt the following values for the total column densities integrated along the line on sight (*i.e.* for the sum of the two components), with 1 σ error bars: $\log N(\mathrm{D\ I}) = 12.88 \pm 0.08$ and $\log N(\mathrm{N\ I}) = 13.35 \pm 0.03$ (cm^{-2}).

The O I column density reported by Hébrard et al. (1999) was obtained using only the saturated 1302 Å line and was inaccurate. In addition, the fit of this line was poor. The new O I column density reported here was obtained from a public set of *FUSE* GI observations of Sirius B (Holberg et al. 2002), which show unsaturated O I absorption lines (see Table 2). Two examples of fits of the O I lines are given in Figure 1.

4.2. *WD 2004−605*

The photometric distance of the DA1 white dwarf WD 2004−605 reported by Holberg et al. (1998) is 52 pc. Three observations of this target were performed as part of the *FUSE* Science Team D/H program. Some exposures were lost due to thermal misalignment of the instrument (for example, the ten first exposures of P2042202), but the final combined spectra have a good signal to noise ratio, with a stellar continuum around $1 - 4 \times 10^{-12}$ erg cm^{-2} s^{-1} Å^{-1}. Numerous unsaturated D I, O I, and N I lines were detected. Neither lines from stellar He II nor interstellar H_2 were detected; thus, the fitting process is quite simple. Examples of four spectral windows are shown in Figure 2-upper panel. O I and N I column densities were measured independently using the curve-of-growth method (Lehner et al. 2003). Both methods (profile fitting and curve-of-growth) gave similar results, and the final values reflect the combined effort of these two analyses.

4.3. *WD 1631+781*

The photometric distance of WD 1631+781 is 67 pc (Holberg et al. 1998). Observed in January 2000, this DA1 white dwarf was the first *FUSE* target for which well resolved Ly-β D I lines were detected. However, Ly-β was the only D I transition observed because, at that time, uncontrolled thermal misalignment of the instrument prevented acquisition of the targets in the MDRS slits of the SiC channels. A new observation performed one year later obtained the shorter wavelength Lyman lines in the SiC channels. Combined spectra of the two observations show numerous unsaturated lines, absorbed on a $\sim 1-5\times10^{-12}$ erg cm^{-2} s^{-1} Å^{-1} simple stellar continuum. No strong H_2 lines were detected, so line blending is not an issue. Four examples of fits are plotted in Figure 2-lower panel. Here again, the O I and N I column densities include input from the independent work by Lehner et al. (2003).

4.4. *CPD−31 1701*

Subdwarfs can yield a high UV flux at distances beyond 100 pc. Thus, they allow the diffuse interstellar medium to be observed on larger path lengths and higher column densities compared to white dwarf sight lines. CPD−31 1701 is a sdO subdwarf which is 131 ± 28 pc from the Sun, according the Hipparcos parallax measurement. This target was observed as part of the *FUSE* Science Team D/H program, through both the LWRS and the MDRS slits. The stellar flux is relatively high, ranging from 2 to 5×10^{-11} erg cm^{-2} s^{-1} Å^{-1}. Numerous unsaturated D I, O I, and N I lines were detected in absorption. Some H_2 lines were also detected, but are excluded from the analysis, due to blends with atomic lines. Similarly, we used only interstellar lines that were not strongly blended with the numerous stellar lines in the spectra.

Comparisons made with stellar models show that blending of the interstellar lines used with stellar lines are not a significant problem, and that fitted polynomials produce acceptable estimates of the continua. An extensive study of the possible effects of stellar models on interstellar column density measurements for lines of sight toward subdwarfs will be the aim of a forthcoming paper. The error bars reported here should be considered as conservative first estimates, and will be refined in a future report. Four examples of fits are given in Figure 3-upper panel.

4.5. *BD +28° 4211*

BD +28° 4211 is a bright sdO subdwarf, located $\sim$ 100 pc from the Sun, *i.e.* at the limit of the Local Bubble (Snowden et al. 1998; Ferlet 1999; Sfeir et al. 1999). The first analysis of *FUSE* spectra of this target was published by Sonneborn et al. (2002), who reported high D/O and low O/H ratios compared with the other *FUSE* lines of sight (Moos et al. 2002). The O/H was also significantly lower than the ratio found by Meyer et al. (1998) for the local interstellar medium. These differences may result from local inhomogeneities in the abundance of oxygen toward that target, but also from under-evaluation of the O I column density (or both). The error bar on N(O I) reported by Sonneborn et al. (2002) was large even though the signal-to-noise ratio was high, primarily because the three O I transitions used are near saturation. As can be seen in their Figure 11, the strongest line (λ 930.3 Å) is the best fitted, while the fit is poor for the less saturated line (λ 919.9 Å). We re-investigated this analysis in order to reduce the error bars, especially on N(O I).

Six extra observations of BD +28° 4211 were performed using all three *FUSE* slit widths (LWRS, MDRS, and HIRS) in July 2001. This added an extra 16.5×10^3 s of exposure time to the 51.6×10^3 s of exposure time for the four observations used by Sonneborn et al. (2002). Although the increase in exposure time is modest, it includes new spectra obtained through the narrowest slit (HIRS). All of the data were processed (or reprocessed) using CalFUSE 2.1. Spectral lines obtained through the three slits and the four channels were fitted simultaneously; the final fit includes 88 spectral windows (four of them are plotted in Figure 3-middle panel.)

As some D I and O I absorption lines are blended with H_2 lines (levels J = 1, 2, and 3), a molecular component was added in the fit, with all of the molecular parameters remaining free to vary. Thus, the final error bars on D I and O I column densities take into account the uncertainties in the H_2 column densities. The D I and N I lines included in our new fits were essentially the same as the ones used in the initial analysis – some extra lines were included but they are weak. The main difference with the analysis of Sonneborn et al. (2002) concerns the O I lines. The transition λ 930.3 Å, which is probably slightly saturated, was not included and we added two extra unsaturated lines, λ 922.2 Å and λ 974.1 Å.

Our new results agree with the initial ones by Sonneborn et al. (2002) at a 1 σ level. The error bars are reduced however, and this sight line now appears to be more in agreement with the other ones in terms of D/O and O/H.

Since the BD +28° 4211 line of sight presents both a high column density and high signal-to-noise ratio observations, it allows inaccurate tabulated f-values of O I lines to be identified. The two O I triplets at 972.14 Å and 1026.47 Å are plotted in Figure 4. Fits were performed following the prescription discussed above, *i.e.* without using these two lines. We see that the f-values tabulated by Morton (1991) for the two lines are clearly overestimated, at least by a factor of 5 and 30 for the λ 972.14 Å and λ 1026.47 Å lines, respectively. The f-values for these two weak intersystem transitions were calculated by Kurucz & Peytremann (1975) and show large error bars. We did not use them for column density measurements toward any target.

4.6. *LSS 1274*

LSS 1274 is a sdO subdwarf, located 580 ± 100 pc from the Sun (Dreizler 1993). Thus, with HD 191877 and HD 195965 (Hoopes et al. 2003), this is one of the three longest lines of sight for which deuterium abundances have been measured with *FUSE*. This star is fainter than the three other subdwarfs presented here; the stellar flux ranges from 1 to 2.5×10^{-12} erg cm^{-2} s^{-1} Å^{-1}. Numerous interstellar lines are detected but most of them are saturated due to the high column density. In addition, numerous H_2 interstellar lines and stellar features are present. We used only the interstellar lines un-blended with stellar features. We included the following species in the fit: D I, O I, N I, Fe II, and the levels $J = 1$ to $J = 5$ of H_2. Four examples of fits are plotted in Figure 3-lower panel.

Finally, λ 974 Å is the only unsaturated O I line that we can use. This makes our O I column density especially dependent on the f-value uncertainty. This is probably the largest value of N(O I) measurable with *FUSE*. Note that O I lines with lower f-values within the *FUSE* range are located at wavelengths shorter than 925 Å, where they are usually undetectable due to blends with the strong H I Lyman lines. Thus, $\log N$(O I) values larger than 17.9 probably will not be measurable with *FUSE*, and will require the λ 1356 Å line in the HST wavelength range.

4.7. *Feige 110*

An extensive study of the Feige 110 sight line was performed by Friedman et al. (2002). We use their D I and O I column densities, together with a new N(N I) value. This latter one was obtained from the data set previously used by Friedman et al. (2002). Due to the numerous stellar and H_2 interstellar lines, most of the N I lines are blended so they do not allow a column density measurement. However, two unsaturated N I lines are detected around 951 Å, which seem un-blended. The corresponding fit is plotted in Figure 5. Only the strongest one is clearly detected. Our result is therefore subject to possible systematic errors, due to an uncontrolled blend or a poorly known oscillator strength. Note that we did not see any of these effects in the case of BD +28° 4211, for which these lines were used, together with other N I lines.

5. RESULTS

The measured column densities as well as the D/O and D/N ratios are displayed in Table 3, sorted from the lowest D I column density to the highest. In addition to the seven targets discussed above, the Table includes 12 targets with previously published *FUSE* analyses (HZ 43 A, G191−B2B, Capella, WD 0621−376, WD 2211−495, WD 1634−573, WD 2331−475, GD 246, HZ 21, Lan 23, HD 191877, and HD 195965), and five other targets with *IMAPS*, HST, and/or *Copernicus* observations (α Vir, δ Ori A, γ Cas, ϵ Ori, and ι Ori). All the references are reported in Table 3. Note that some of the column densities for the four latter targets were obtained using only one transition, which make them more dependent on possible inaccuracies in the atomic data. For the case of the HST measurements of N(O I) reported by Meyer et al. (1998), we corrected the values with an updated

oscillator strength for the transition used ($\lambda\,1356$ Å), in agreement with Meyer (2001). Altogether, a sample of 24 lines of sight with D I, O I, and N I interstellar column densities is available. We did not include lines of sight with published D/H but without known D/O.

York (1983) has measured the column density for D I, O I, and N I towards λ Sco. The total D/O value is low but presents large variations from component to component. There is a possibility the uncertainties should be larger due to the use of saturated lines. In addition, although the star is $\sim$ 220 pc (Hipparcos parallax measurement), the Local Bubble wall has protrusions and appears porous in that general direction (Lallement et al. 2003), so the location of the gas measured is quite uncertain. Therefore, we have not included this line of sight in our sample.

Figure 6 presents the D/O and D/N ratios as a function of the D I column density. For the targets with the lowest D I column densities, *i.e.* for the near local interstellar medium (LISM), the D/O ratio appears to be remarkably constant, contrary to D/N. For the 14 targets with $\log N(\mathrm{D\ I}) \leq 14.5$, we obtained the weighted mean $\mathrm{D/O} = (3.84 \pm 0.16) \times 10^{-2}$ (all the means reported here are weighted by the reported errors). The ± 0.16 error that we report here and the errors that we report below are $1\,\sigma$ uncertainties in the mean. Note that the square root of the weighted average variance, which may be used to compare a single new measurement with the mean, is ± 0.49. The χ^2 for this weighted mean is 8.4 for 13 degrees of freedom; the data are consistent with a single value for the the D/O ratio in the near LISM, which is probably the Local Bubble. In comparison, for the same 14 targets, the χ^2 for the weighted mean of D/N is 37.3, indicating that D/N varies more significantly from one line of sight to the other. At higher D I column densities, both the D/O and D/N ratios vary. The weighted means and the χ^2 for all the sight lines are respectively 3.05×10^{-2} and 117.9 for D/O, and 1.90×10^{-1} and 189.9 for D/N, for 23 degrees of freedom.

In order to better examine variations of the D/O ratio in different regions of the LISM, we plot it as a function of the Galactic latitude and distance in Figure 7. The sample contains only a few high latitude stars and most of them are close with modest D I column densities. Thus, it is not surprising that the scatter is limited. However, the D/O values near the Galactic plane, which correspond to a wide range of D I column densities, show a larger scatter, in agreement with the variation as a function of column density discussed above. As a function of the distance, D/O is homogeneous on lines of sight toward stars of 150 pc or less. For the 16 targets in that range, we find $\mathrm{D/O} = (3.96 \pm 0.15) \times 10^{-2}$, with a χ^2 of 12.5 for 15 degrees of freedom. So, again, there is no evidence for variation of D/O in the LISM, even to distances slightly outside the Local Bubble.

We plot in Figure 8 the reduced χ^2 of the D/O weighted mean as a function of the D I column density and as a function of the target distances, which serve as upper limits for the distance to the ISM gas. The χ^2 values remain similar to the degrees of freedom (reduced χ^2 near unity) for distances lower than 150 pc and $N(\mathrm{D\ I}) < 15$, but the values increase significantly above these limits as the D/O values deviate more and more from the low-distance and low-column density mean. We can not draw strong conclusions about D/O variations or homogeneity in the range $14.5 < \log N(\mathrm{D\ I}) < 15$, because we have only one target (BD $+28^\circ$ 4211). Thus, we adopt $\log N(\mathrm{D\ I}) \leq 14.5$ as a conservative cutoff for the D/O homogeneity. Using a D/H ratio ranging between 1.3 and 1.5×10^{-5} (see Sect.6.2), this cutoff corresponds to $\log N(\mathrm{H\ I}) = 19.3 - 19.4$, which is the value used by Sfeir et al. (1999) for the wall of the Local Bubble. In comparison to D/O, D/N shows variability at lower distances and D I column densities (Figure 8). The D/N variations are actually detected as soon as a few targets are included in the sample. We have also examined the reduced χ^2 starting with the maximum values of D I column density and target distances, *i.e.* from right to left. For both D/O and D/N, after a few points the reduced χ^2 takes on a value greater than one, indicating variability at large distances and column densities.

Some of the distances are photometric, with no error bars reported and should be regarded as uncertain. In Figure 7, we assumed a 30 % uncertainty for such cases, but this may be an underestimation. For example, in the case of CPD$-31\,1701$, Bauer & Husfeld (1995) reported a photometric distance of 320 ± 80 pc, while the Hipparcos measured parallax of 7.62 ± 1.51 mas is equivalent to 131 ± 28 pc. Moreover, the distances are those of the stars, and are only upper limits for the distances to the interstellar gas. We prefer to define the local interstellar medium in terms of column density. Thus, we adopt the D/O ratio obtained with the D I column density criterion rather than distance criterion, and we report the following value for the D/O ratio in the Local Bubble from *FUSE* observations with $\log N(\mathrm{D\ I}) \leq 14.5$:

$$(\mathrm{D/O})_{\mathrm{LB}} = (3.84 \pm 0.16) \times 10^{-2} \quad (1\,\sigma).$$

This result, which is obtained from 14 lines of sight, is in agreement with the earlier *FUSE* results: Moos et al. (2002) and Oliveira et al. (2003) reported $(\mathrm{D/O})_{\mathrm{LB}} = (3.76 \pm 0.20) \times 10^{-2}$ and $(\mathrm{D/O})_{\mathrm{LB}} = (3.87 \pm 0.18) \times 10^{-2}$ for 5 and 8 lines of sight, respectively. The increased number of sight lines further reduces the uncertainty.

6. DISCUSSION

We discuss here the above results. The various deuterium abundance values discussed below are summarized in Table 4.

6.1. *D/O and D/H homogeneities in the LISM*

The D I and O I column densities differ by less than two orders of magnitude. Hence, as discussed previously, systematic errors in D/O are likely to be smaller than those associated with the determination of D/H. Moreover, any residual systematic over- or underestimation of our column densities, due for example to subtle effects in the LSF, zero flux level estimates, or line of sight velocity structures, will be reduced when taking the ratio of $N(\mathrm{D\ I})$ to $N(\mathrm{O\ I})$. According to the above effects, this is probable that part of the errors for $N(\mathrm{D\ I})$ and $N(\mathrm{O\ I})$ are correlated. However the errors are combined with the conservative assumption they are independent. This tends to slightly overestimate the error bars on D/O and may be why the reduced χ^2 for the Local Bubble is less than one. Thus, it is likely that the results for D/O are robust.

The homogeneity of D/O in the near LISM argues against variations of D/H in the Local Bubble. Indeed, the only possible way that D/O could be stable while D/H varies, would be for D/H and O/H to be correlated. Moreover, they would have to vary in a precise manner that allowed D/O to remain constant. That seems improbable for two *different* reasons: (i) O/H appears to be uniform in the ISM over paths of several hundred parsecs (*e.g.*, Meyer et al. 1998), and (ii) astration processes should lead to an anti-correlation of D I and O I abundances. Thus, the stability of D/O in the near LISM is a strong argument for the stability of both D/H and O/H in the Local Bubble.

Conversely, the variations of D/O from one sight line to the other for distances greater than 150 pc and D I column densities larger than 10^{15} cm^{-2} is an argument which supports D/H variations at these scales, as studies by Meyer et al. (1998), Cartledge et al. (2001), or André et al. (2003) show that the O/H ratio does not vary significantly over the distances covered in this study. Thus, while the interstellar medium seems well mixed inside the Local Bubble, this is not the case beyond 150 pc. It appears that D/O varies from sight line to sight line, whereas the studies above show that O/H does not. A comparison between the interstellar values and the low-metallicity quasar sight lines values shows that D I and O I are, at least partially, anti-correlated over large ranges in the metallicity. However, for most of the distant ISM targets studied here, the mechanisms affecting D I do not appear to affect O I significantly. This will provide a constraint on mixing models (*e.g.*, de Avillez & Mac Low 2002) and chemical evolution models (*e.g.*, Chiappini et al. 2002).

Because of the variations in the D/O ratio outside of the Local Bubble, it is difficult to choose which value for D/O is representative of the present epoch. There certainly is no reason to preferentially adopt the D/O value measured in the Local Bubble. Note a possible trend; the D/O values are lower for the higher D I column densities and especially the larger distances (Figures 6 and 7). Consider the three farthest targets, both in terms of distance and column density (namely LSS 1274, HD 191877, and HD 195965). Their D/O ratios are low, with a weighted average value of D/O = $(1.50\pm0.25)\times10^{-2}$. This is 2.5 times lower (shifted by $9\,\sigma$) than the local value, D/O = $(3.84 \pm 0.16) \times 10^{-2}$. This result is based on only 3 points, and must be accepted with caution. However, an examination of Table 3 shows that most of the targets with distances approximately $\geq$ 200 pc have low values of D/O, Feige 110 being the primary exception. In addition, the three targets discussed above, all more distant than $\sim$ 500 pc and with D I column densities larger than 7×10^{15} cm^{-2}, are in different directions (see Table 3) and hence, probe different media. This result suggests the present-epoch D/O ratio is lower than 3.84×10^{-2}. The reason for a high local value is uncertain, but the possibility of unknown deuterium enrichment process(es) must be considered. A detailed discussion of such enrichment mechanisms is outside the scope of this report.

It could be argued that the low values of D/O are due to undetected saturated components. In the case of HD 195965 and HD 191877 Hoopes et al. (2003) found that high-resolution ground based K I data suggested that there were no narrow unresolved features on either sight line and when they used their STIS data for HD 195965, they were able to show this more conclusively for that sight line. Similar data does not exist for LSS 1274. Generally the heavier O I absorption features should saturate before the D I features, as at least a part of the line broadening is thermal. Thus, one would expect that on average, such effects should tend towards increased values rather than decreased values as is reported here. γ Cas, ϵ Ori, and ι Ori may be exceptions to this argument in that N(D I) was measured by *Copernicus*, but the HST determination of N(O I) used the weak intercombination transition at λ 1356 Å.

6.2. *Local D/H value inferred from D/O*

The accurate D/O ratio determined for the Local Bubble can be used to estimate D/H in the Local Bubble, if the value of O/H is known. By assuming the Meyer et al. (1998) value as updated by Meyer (2001), O/H = $(3.43\pm0.15)\times10^{-4}$, we obtain $(\mathrm{D/H})_{\mathrm{LISM}} = (1.32\pm0.08)\times 10^{-5}$ $(1\,\sigma)$. This value is about 15 % lower than the average values $(\mathrm{D/H})_{\mathrm{LISM}} = (1.5 \pm 0.1) \times 10^{-5}$ $(1\,\sigma)$ obtained by Linsky (1998) from the comparison of HST data for 12 nearby sight lines, and $(\mathrm{D/H})_{\mathrm{LISM}} = (1.52 \pm 0.08) \times 10^{-5}$ $(1\,\sigma)$ obtained by Moos et al. (2002) for the first five lines of sight observed with *FUSE*. Although the difference with these direct measurements is about $2\,\sigma$, which is marginally significant, it is reassuring that D/H derived from direct and indirect measurements are so close, lending assurance that the values presently used for the Local Bubble are at least approximately correct.

What is the source of the disagreement between the two values? It is possible that at least one of the three measurements, the D/O (this study), the D/H (Linsky 1998; Moos et al. 2002), and the O/H (Meyer et al. 1998), is slightly under- or overestimated.

In a similar manner, using the Meyer et al. (1998) O/H value, the Linsky (1998) and Moos et al. (2002) D/H values predicts D/O = $(4.4 \pm 0.3) \times 10^{-2}$ $(1\,\sigma)$. The deduced value is high by about $2\,\sigma$.

This disagreement could be due to the O/H value of Meyer et al. (1998), which was obtained from GHRS observations of 13 lines of sight ranging from 130 to 1500 pc, most of them being closer than 500 pc. The Meyer et al. study deals with interstellar clouds that are more distant than the upper limit we found for the extent of the region in which D/O was homogeneous: $\sim$ 150 pc. However, the O/H value given by Meyer et al. (1998) agrees with that measured in the more local ISM by Moos et al. (2002) and Oliveira et al. (2003) with *FUSE*. In order for both D/O and D/H to be respectively 3.8×10^{-2} and 1.5×10^{-5}, the value of O/H in the Local Bubble would have to be as high as 3.9×10^{-4}. A local enrichment of oxygen in the interstellar gas could exist if the depletion onto dust grains is lower (see Sect. 6.5). However, as discussed above, measurements of O/H for nearby gas do not show any evidence for such an enrichment. Note that systematic errors at the 15 % level in the atomic data cannot be ruled out. The Meyer et al. study used one O I transition (λ 1356 Å) whereas the *FUSE* measurements for the Local Bubble used transitions in the *FUSE* wavelength range. The two sets of oscillator strengths have not been compared with sufficient precision to eliminate this possibility.

Finally, one might ask if the disagreement could be caused by slight inaccuracies in the local D/H values caused by unknown systematic errors in the determination of the H I column densities. Vidal-Madjar & Ferlet (2002) suggested that direct measurements of D/H in the very local ISM ($\log N(\mathrm{H\ I}) < 10^{19}$ cm^{-2}) could be underestimated by as much as $\sim$ 20 %. They suggested broad weak components in the interstellar gas that could lead to *overestimates* of N(H I), but would be undetectable for the much lower D I column densities. However, the Local Bubble D/H ratio deduced here from D/O is lower than the direct measurements. This suggests that this effect is not prevalent for most sight lines in the Local Bubble, although the possibility that it exists for a few sight lines cannot be ruled out.

6.3. *Evidence for a low present-epoch D/H*

In this study, a D/H ratio of $(1.32 \pm 0.08) \times 10^{-5}$ was estimated for the Local Bubble, and variations start to occur beyond $\sim$ 150 pc. At larger distances, there appears to be a downward trend in the values of D/O. We reported above that the weighted average for the three farthest targets of our sample yields a low D/O ratio, $(1.50 \pm 0.25) \times 10^{-2}$. Using the Meyer et al. (1998) O/H ratio, this D/O translates into D/H = $(5.2 \pm 0.9) \times 10^{-6}$ ($1\,\sigma$). This value is significantly lower than the ones usually assumed, by a factor much larger than the 15 % shift found for the Local Bubble in the comparison above. Although local material has a higher D/H ratio, raising the sight line integrated values, the effect will be slight because the local column densities are so much smaller. It is possible that the hint of anti-correlation between D/H and O/H, which was claimed by Steigman (2003) from a study of the first *FUSE* results presented by Moos et al. (2002), would yield slightly higher O/H ratios on average for these distant sight lines, and hence, would increase the value of D/H. However, as noted above, O/H is generally homogeneous over the distances covered in this study and if there is an increase, it likely is not strong enough to increase the value deduced for distant gas to the local D/H ratio.

While high values of D/H (above 2×10^{-5}) have been reported toward two distant targets, namely γ^2 Vel (Sonneborn et al. 2000) and Feige 110 (Friedman et al. 2002), five low values of D/H (below 1×10^{-5}) were also previously reported toward distant targets with *Copernicus*, *IMAPS*, or *FUSE*: δ Ori A (Laurent et al. 1979; Jenkins et al. 1999), λ Sco (York 1983), θ Car (Allen et al. 1992), and HD 191877 and HD 195965 (Hoopes et al. 2003). Values of D/H below 1×10^{-5} were also measured in two Orion regions through ISO observation of HD (Bertoldi et al. 1999; Wright et al. 1999). If the present-epoch D/H is actually below 1×10^{-5}, as is suggested here, it might require high deuterium destruction factors for astration processes (see Sect. 6.6).

6.4. *D/N ratio: ionization*

Whereas D/O is homogeneous for distances less than 150 pc and D I column densities lower than 1×10^{15} cm^{-2}, the D/N ratio varies significantly in the near local interstellar medium. The difference is likely due to the fact that for sufficiently low H I column densities, O I is a better tracer of H I than N I because of ionization effects. G191−B2B is an example of a local line of sight where nitrogen is not a good hydrogen tracer (Vidal-Madjar et al. 1998). Nitrogen is likely to be more ionized than hydrogen, whereas oxygen and hydrogen are more strongly coupled to each other by charge exchange reactions (Sofia & Jenkins 1998; Jenkins et al. 2000). If ordinary recombination with free electrons dominates over the charge exchange reaction of N II with H I, we expect to have $n_{\mathrm{N\,II}}/n_{\mathrm{N\,I}} > n_{\mathrm{H\,II}}/n_{\mathrm{H\,I}}$, since the N I photo-ionization cross section is larger than that of H I (Hébrard et al. 2002). This inequality with the hydrogen ionization fraction does not arise for oxygen because the charge exchange cross section of O II with H I is considerably larger than for N II with H I. Thus, as a substantial fraction of the LISM is partially ionized in the Local Bubble, N(D I)/N(N I) is not a good approximation for D/N. Indeed, N II has abundances similar to those of N I in the Local Bubble (see, *i.e.*, Wood et al. 2002b) and there are even at least three targets for which N(N II) > N(N I): HZ 43 A (Kruk et al. 2002), WD 1634−573 (Wood et al. 2002a), and WD 2211−495 (Hébrard et al. 2002).

In addition, if N(N II)/N(N I) varies because of an inhomogeneous flux of EUV photons, the N(D I)/N(N I) ratio may also vary, being higher toward the most ionized regions. Tests on species highly dependent on ionization, like Ar I, or on ratios such as N(Si II)/N(Si I), may help to determine if there is a correlation between ionization and the D/N variations which we detected. This is beyond the scope of the present work on D/O. For a study of ionization conditions in the Local Bubble and the LISM slightly beyond, see Slavin & Frisch (2002) or Lehner et al. (2003).

The problem of nitrogen ionization is less critical outside the Local Bubble, where the N/H ratio has been shown to be homogeneous for H I column densities $\geq 1 \times 10^{20}$ cm^{-2} (Ferlet 1981; Meyer et al. 1997).

For high column densities, the D/N ratio may be a valuable D/H proxy, although it will not be as secure as D/O until more extensive studies of the chemical abundances of N I in the ISM are performed. Figure 9 shows the D/O as a function of the D/N ratio for our sample. A correlation seems to appear, but with large scatter; the lowest D/N ratios are generally measured toward targets with low D/O ratios. These are also the more distant targets. The one exception is Feige 110 with a high D/O and a highly uncertain distance between 112 and 444 pc. This correlation can be understood in part by noting that at low column densities, the D/O ratio is higher than average and the D/N ratio is also higher due to ionization effects, whereas at high column densities, we have found D/O to be lower and D/N is also expected to decrease as the effects of EUV ionization falls off.

The weighted average of D/N for the three farthest targets (LSS 1274, HD 191877, and HD 195965) is D/N = $(1.15 \pm 0.16) \times 10^{-1}$, without significant variations. Assuming the N/H ratio measured by Meyer et al. (1997), N/H = $(7.5 \pm 0.4) \times 10^{-5}$, our D/N ratio for distant gas yields D/H = $(8.6 \pm 1.3) \times 10^{-6}$ ($1\,\sigma$). This is not in perfect agreement with the D/H ratio obtained through D/O; the error bars overlap at the $2\,\sigma$ level. This could be caused by ionization and/or variations in the chemical abundance. In any case, this value is significantly lower than the D/H

value usually assumed for the present epoch.

6.5. *Oxygen depletion*

Whereas the D I column density represents the total amount of neutral deuterium in the interstellar medium observed here, this is not the case for O I. A significant fraction of the interstellar oxygen is depleted onto dust grains, and this amount does not contribute to the measured absorption. Cardelli et al. (1996) estimated the relative amount of oxygen in the solid phase to be $O/H \simeq 1.8 \times 10^{-4}$. Thus, in addition to the gaseous oxygen measured by Meyer et al. (1998), $O/H \simeq 3.4 \times 10^{-4}$, the total interstellar oxygen should be $O/H \simeq 5.2 \times 10^{-4}$. This value agrees with the Solar value obtained by Allende Prieto et al. (2001): $O/H = (4.9 \pm 0.6) \times 10^{-4}$ (a lower value than the ones previously reported). Thus, about one third of the total oxygen is depleted onto dust grains.

When using our D/O measurement, one considers only the gas phase abundance of the neutral oxygen. However, the same holds when using the O/H interstellar measurement, so no depletion corrections need to be applied in order to translate a D/O result into a D/H measurement. More importantly, studies by Meyer et al. (1998), Cartledge et al. (2001), and André et al. (2003) have shown that the O/H ratio does not vary and hence, oxygen depletion is constant out to distances of more than 1 kpc, over a wide range of fractional H_2 abundances and H I column densities. Cartledge et al. (2001) found lower oxygen abundances in a few translucent clouds on the line of sight to distant stars. This first hint of oxygen depletion enhancement should imply an increased value of the D/O for sight lines of this type. However, those lines of sight were much denser than the ones reported here, in which molecular hydrogen is at most a few percent, and generally less than 10^{-4} of the H I column.

6.6. *Deuterium evolution*

There are primarily two ways to examine the evolution of the abundance of deuterium throughout the history of the Universe: first, from Galactic abundance gradients, and second, from abundances at different stages of evolution (*i.e.* studies of the interstellar *vs.* intergalactic media).

The Galactic abundance gradients are obtained in models of chemical evolution, assuming a radially dependent star formation rate and a timescale for formation of the disk by infall that depends on the galactocentric distance (see, *e.g.*, Hou et al. 2000). Inside-out formation of the Galaxy is also suggested by more sophisticated dynamical models (see, *e.g.*, Samland & Gerhard 2003). As astration destroys deuterium and produces oxygen, the deuterium abundance should be lower in the inner part of the Galaxy compared to the outer part, and oxygen more abundant in the inner part than in the outer. Thus, the D/O ratio should have an even steeper gradient, from low values in the center to high values in the outer part of the Galaxy.

From their "two-infall model", Chiappini et al. (2002) predict the galactocentric gradient $d\log(D/O)/dR \simeq 0.13$ dex/kpc. Assuming that the local value, $D/O = (3.84 \pm 0.16) \times 10^{-2}$, reported here is typical of this region of the Galaxy implies D/O ratios $\sim 2.8 \times 10^{-2}$ and $\sim 5.2 \times 10^{-2}$ should be observed in 1 kpc distant clouds toward respectively the center and the anticenter of the Galaxy. Given our typical error bars, such gradients are detectable with *FUSE*. They should appear as a correlation of the D/O ratio with the Galactic longitude, especially for the distant targets. Up to now, we have not detected such a signature, but our sample of distant targets is still poor: only five targets could be more distant than 500 pc.

We note that Chiappini et al. (2002) predict a D/O value between $\sim 2.5 \times 10^{-2}$ and $\sim 4.0 \times 10^{-2}$ at a galactocentric distance of 8 kpc, *i.e.* the distance of the LISM. Because the value predicted by Chiappini et al. (2002) refers to all the oxygen, *i.e.* even that which is depleted on the dust grains, it is necessary to decrease the value for the Local Bubble, $D/O = (3.84 \pm 0.16) \times 10^{-2}$, by about 30 %. The total local D/O is then around 2.7×10^{-2}, in agreement with the value predicted by Chiappini et al. (2002). Note that the value of D/H in the Local Bubble may be high compared to other regions, as discussed above.

Abundance measurements at different stages of evolution are the second way to constrain the evolution of deuterium. Whereas the abundances in the interstellar medium are representative of the present epoch, primordial abundances likely exist in the intergalactic low-metallicity clouds observed towards quasars at high redshifts. These values for the primordial abundance may also be compared with those deduced independently from the cosmic microwave background (CMB) anisotropy studies (see, *e.g.*, Cyburt et al. 2003; Spergel et al. 2003). Primordial D/H values between 2.5 and 3.0×10^{-5} are the preferred ones, as they are observed toward several quasars (O'Meara et al. 2001; Kirkman et al. 2003) and they are in quite good agreement with CMB measurements performed with different missions such as BOOMERANG (de Bernardis et al. 2002), DASI (Pryke et al. 2002), ARCHEOPS (Benoît et al. 2003), or now WMAP (Bennett et al. 2003). These measurements imply a baryon-to-photon ratio around $\eta \sim 6 \times 10^{-10}$. Note however, the different results from MAXIMA (Stompor et al. 2001), the high D/H measurement reported by Webb et al. (1997), and the fact that the baryonic density inferred from the low D/H values through BBN is not in good agreement with those based on helium and lithium primordial abundances.

Standard chemical evolution models predict a D/H decrease by a factor 2 to 3 in 15 Gyrs (*e.g.*, Galli et al. 1995; Prantzos 1996; Tosi et al. 1998). More recent models predict smaller decreases, by factors ~ 1.5 (Chiappini et al. 2002). With such low factors, it becomes more difficult to link the primordial D/H measurements, found to be between 2.5 and 3.0×10^{-5}, with the one we deduced here for the local interstellar medium, around 1.3×10^{-5}. The problem becomes more severe if the present-epoch D/H is below 1×10^{-5}, as suggested above. Note however that there are some nonstandard models which propose higher astration ratios (Vangioni-Flam & Cassé 1995; Scully et al. 1997).

In addition, the estimates of the proto-solar abundances of deuterium favor values of D/H around $2-3 \times 10^{-5}$ (Gautier & Morel 1997; Mahaffy et al. 1998; Lellouch et al. 2001, Hersant et al. 2001), *i.e.* near the primordial ones. This result allows only low astration factors during the first ten

Gyears, most of the astration occurs in the recent Universe. Such assumptions jeopardize standard models.

Up to now, only a few measurements of deuterium in primordial media have been made. In QSO 1937−1009 and QSO 1009+2956, Burles & Tytler (1998a; 1998b) reported D I detections which allow measurements of the primordial D/H, but they obtained only upper limits on the O I column densities. O'Meara et al. (2001) presented the first simultaneous measurements of D I and O I column densities toward the $z \simeq 2.5$ Lyman limit system on the line of sight to QSO 0105+1619 and obtained D/O = $(280 \pm 30) \times 10^{-2}$. Levshakov et al. (2002) reported also an O I detection in the $z \simeq 3.0$ damped Ly-α system toward QSO 0347−3819, in which D'Odorico et al. (2001) previously reported a D I measurement. That new study yields the following value: D/O = $(37 \pm 3) \times 10^{-2}$. Note that when using the initial D'Odorico et al. (2001) N(D I) measurement, that ratio is reduced to D/O = $(21 \pm 4) \times 10^{-2}$. Finally, Kirkman et al. (2003) recently detected both D I and O I in a third intergalactic cloud, at a redshift $z \simeq 2.5$ toward the quasar QSO 1243+3047. They found a high ratio: D/O = $(3000 \pm 300) \times 10^{-2}$ (all the error bars given here are within a $1\,\sigma$ confidence interval). Thus, the few primordial D/O measurements available are significantly higher than our local interstellar D/O value. The local D/O is decreased by factors between ~ 5 and ~ 70 with respect to the primordial ones, and even by a factor as high as ~ 800 when compared to the high D/O value reported by Kirkman et al. (2003). This result confirms that D/O is a very sensitive probe of astration. According to Chiappini et al. (2002), the D/O values predicted in the outer parts of the Galaxy should be close to the primordial value. From their model, they computed D/O values between $\sim 25 \times 10^{-2}$ and $\sim 100 \times 10^{-2}$ for galactocentric distances between 15 and 18 kpc, respectively.

7. CONCLUSION

We have presented the first results of a *FUSE* survey of D/O in the interstellar medium. D/O is a good D/H proxy because it does not require ionization or significant depletion corrections. Using oxygen instead of hydrogen also reduces the systematic errors for the measured column densities. Only six D/O measurements were available prior to the *FUSE* mission; the present sample totals 24 lines of sight.

We find that the D/O ratio is homogeneous in the near local interstellar medium, with a weighted mean D/O = $(3.84 \pm 0.16) \times 10^{-2}$ (~ 4 % uncertainty in the mean at $1\,\sigma$). This value is representative of the interstellar medium in the Local Bubble, for distances < 150 pc and $\log N$(D I) ≤ 14.5. The remarkable homogeneity of D/O is a strong argument for both D/H and O/H stability at the scale of the Local Bubble.

The local D/O value and the average value of O/H in the local interstellar medium obtained by Meyer et al. (1998) imply that $(\mathrm{D/H})_{\mathrm{LISM}} = (1.32 \pm 0.08) \times 10^{-5}$. This value is slightly lower than the values obtained from direct D/H measurements in the Local Bubble ($(1.52 \pm 0.08) \times 10^{-5}$; Moos et al. 2002) or the Local Interstellar Cloud ($(1.5 \pm 0.1) \times 10^{-5}$; Linsky 1998). Linking these local values with the primordial ones is marginal if astration factors around 1.5 (Chiappini et al. 2002) are used. Using a low deuterium astration factor of 1.5, our local D/H value translates into a primordial value around 2×10^{-5}. According to the standard Big Bang Nucleosynthesis predictions, this corresponds to a baryon-to-photon ratio around $\eta = 7.2 \times 10^{-10}$, slightly higher than most of the determinations made from the anisotropy of the cosmic microwave background.

Beyond the Local Bubble, we found significant variations in the value of D/O, implying D/H variations. In addition, the D/O values are typically lower. Indeed, the more distant targets suggest a present-epoch deuterium abundance below 1×10^{-5}, *i.e.* lower than the value usually assumed. As these sight lines are in different directions on the sky, it follows that the local value of D/H may be high compared to other nearby regions in the Galaxy.

We did not detect any correlation between the target-to-target variations and the changes with galactic longitude expected to result from predicted galactocentric abundance gradients. However, the number of distant targets is quite small and additional D/O studies of distant lines of sight will be needed to detect such gradients. Together with N(H I) estimations, additional measurements would also shed light on the hint of anti-correlation between D/H and O/H reported by Steigman (2003). Finally, additional studies of distant sight lines will confirm or disprove the evidence for low deuterium abundance in the present epoch implied by the date reported here. If the low D/O values measured at large distances are representative of the present-epoch value, rather than the local one, this would further increase the difficulty in linking the present and primordial deuterium abundance values through astration correction.

This work is based on data obtained by the NASA-CNES-CSA *FUSE* mission operated by the Johns Hopkins University. Financial support to H.W.M. was provided by NASA contract NAS5-32985. G.H. was supported by CNES. This work used the profile fitting procedure Owens.f developed by M. Lemoine and the French *FUSE* Team. We would like to thank D. C. Morton for useful comments about atomic data, J.-M. Désert, S. Lacour, and A. Moullet for their help in data processing, and E. Vangioni-Flam and S. Boissier for useful discussions.

This study is part of a extensive program in which all of the D/H Working Group of the FUSE Principal Investigator Team participated. We especially acknowledge M. K. André, W. P. Blair, P. Chayer, J. Dupuis, R. Ferlet, S. D. Friedman, C. Gry, C. G. Hoopes, J. C. Howk, E. B. Jenkins, D. C. Knauth, J. W. Kruk, A. Lecavelier des Étangs, N. Lehner, M. Lemoine, J. L. Linsky, C. M. Oliveira, K. R. Sembach, J. M. Shull, G. Sonneborn, P. Sonnentrucker, T. M. Tripp, A. Vidal-Madjar, G. M. Williger, B. E. Wood, and D. G. York. We thank them for many discussions and comments with respect to the deuterium studies.

REFERENCES

Abgrall, H., Roueff, E., Launay, F., Roncin, J. Y., & Subtil, J. L. 1993, A&AS, 101, 323
Abgrall, H., Roueff, E., Launay, F., Roncin, J. Y., & Subtil, J. L. 1993, A&AS, 101, 273
Allen, M. M., Jenkins, E. B., & Snow, T. P. 1992, ApJS, 83, 261
Allende Prieto, C., Lambert, D. L., & Asplund, M. 2001, ApJ, 556, L63
André, M. K. et al. 2003, ApJ, in press (astro-ph/0303586)
Bauer, F., & Husfeld, D. 1995, A&A, 300, 481
Benoît, A. et al. 2003, A&A, in press (astro-ph/0210306)
Bennett, C. L. et al. 2003, submitted to ApJ (astro-ph/0302207)
Bertoldi, F., Timmermann, R., Rosenthal, D., Drapatz, S., Wright, C. M. 1999, A&A, 346, 267
Burles, S., & Tyler, D.: 1998a, ApJ 499, 699
Burles, S., & Tyler, D.: 1998b, ApJ 507, 732
Cardelli, J. A., Meyer, D. M., Jura, M., & Savage, B. D. 1996, ApJ, 467, 334
Cartledge, S. I. B., Meyer, D. M., Lauroesch, J. T., & Sofia, U. J. 2001, ApJ, 562, 394
Chiappini, C., Renda, A., & Matteucci, F. 2002, A&A, 395, 789
Cyburt, R. H., Fields, B. D., & Olive, K. A. 2003, in preparation (astro-ph/0302431)
de Avillez, M. A., & Mac Low, M.-M. 2002, ApJ, 581, 1047
de Bernardis, P. et al. 2002, ApJ, 564, 559
D'Odorico, S., Dessauges-Zavadsky, M., & Molaro, P. 2001, A&A, 368, L21
Dreizler, S. 1993, A&A, 273, 212
Ferlet, R., York, D. G., Vidal-Madjar, A., & Laurent, C. 1980, ApJ, 242, 576
Ferlet, R. 1981, A&A, 98, L1
Ferlet, R. 1999, A&A Rev., 9, 153
Friedman, S. D. et al. 2002, ApJS, 140, 37
Galli, D., Palla, F., Ferrini, F., & Penco, U. 1995, ApJ, 443, 536
Gautier, D. & Morel, P. 1997, A&A, 323, L9
Hébrard, G., Mallouris, C., Ferlet, R., Koester, D., Lemoine, M., Vidal-Madjar, A., & York, D. 1999, A&A, 350, 643
Hébrard, G. et al. 2002, ApJS, 140, 103
Hersant, F., Gautier, D., & Huré, J. 2001, ApJ, 554, 391
Hibbert, A., Dufton P. L., & Keenan F.P. 1985 MNRAS, 213, 721
Holberg, J. B., Barstow, M. A., & Sion, E. M. 1998, ApJS, 119, 207
Holberg, J. B., Kruk, J. W., Barstow, M. A., Burleigh, M. R., Koester, D., Sahu, M. S. 2002, *FUSE* Science and Data Workshop, JHU, Baltimore, 56
Hoopes, C. G., Sembach, K. R., Hébrard, G., Moos, H. W., & Knauth, D.C. 2003, ApJ, 586, 1094
Hou, J. L., Prantzos, N., & Boissier, S. 2000, A&A, 362, 921
Hubeny, I. & Lanz, T. 1995, ApJ, 439, 875
Jenkins, E. B., Tripp, T. M., Woźniak, P. ;. A., Sofia, U. J., & Sonneborn, G. 1999, ApJ, 520, 182
Jenkins, E. B. et al. 2000, ApJ, 538, L81
Kirkman, D., Tytler, D., Suzuki, N., O'Meara, J. M., Lubin, D., 2003, submitted to ApJS (astro-ph/0302006)
Kruk, J. W. et al. 2002, ApJS, 140, 19
Kurucz, R. L., & Peytremann, E. 1975, Smithsonian Astrophysical Obs. Spec. Rept. 362
Lallement, R., Welsh, B. Y., Vergeley, J. L., Crifo, F., & Sfeir, D. 2003, A&A, submitted
Laurent, C., Vidal-Madjar, A., & York, D. G. 1979, ApJ, 229, 923
Lehner, N., Gry, C., Sembach, K. R., Hébrard, G., Chayer, P., Moos, H. W., Howk, J. C., & Désert, J.-M. 2002, ApJS, 140, 81
Lehner, N., Jenkins, E. B., Gry, C., Moos, H. W., Chayer, P., & Lacour, S. 2003, ApJ, in press (astro-ph/0306280)
Lellouch, E., Bézard, B., Fouchet, T., Feuchtgruber, H., Encrenaz, T., & de Graauw, T. 2001, A&A, 370, 610
Lemoine, M. et al. 1999, New Astronomy, 4, 231
Lemoine, M. et al. 2002, ApJS, 140, 67
Levshakov, S. A., Dessauges-Zavadsky, M., D'Odorico, S., & Molaro, P. 2002, ApJ, 565, 696
Linsky, J. L. & Wood, B. E. 1996, ApJ, 463, 254
Linsky, J. L. 1998, Space Science Reviews, 84, 285
Mahaffy, P. R., Donahue, T. M., Atreya, S. K., Owen, T. C., & Niemann, H. B. 1998, Space Science Reviews, 84, 251
Meyer, D. M., Cardelli, J. A., & Sofia, U. J. 1997, ApJ, 490, L103
Meyer, D. M., Jura, M., & Cardelli, J. A. 1998, ApJ, 493, 222
Meyer, D. M. 2001, XVIIth IAP Colloquium, Paris, Edited by R. Ferlet et al., p. 135
Moos, H. W. et al. 2000, ApJ, 538, L1
Moos, H. W. et al. 2002, ApJS, 140, 3
Morton, D. C. 1991, ApJS, 77, 119
Morton, D. C. 2003, in preparation
Oliveira, C. M., Hébrard, G., Howk, J. C., Kruk, J. W., Chayer, P., Moos, H. W. 2003, ApJ, 587, 235
O'Meara, J. M., Tytler, D., Kirkman, D., Suzuki, N., Prochaska, J. X., Lubin, D., & Wolfe, A. M. 2001, ApJ, 552, 718
Perryman, M. A. C. et al. 1997, A&A, 323, L49
Prantzos, N. 1996, A&A, 310, 106
Pryke, C., Halverson, N. W., Leitch, E. M., Kovac, J., Carlstrom, J. E., Holzapfel, W. L., & Dragovan, M. 2002, ApJ, 568, 46
Sahnow, D. J. et al. 2000, ApJ, 538, L7
Samland, M. & Gerhard, O. E. 2003, A&A, 399, 961
Scully, S. T., Cassé, M., Olive. K. A., & Vangioni-Flam, E. 1997, ApJ, 476, 521
Sfeir, D. M., Lallement, R., Crifo, F., & Welsh, B. Y. 1999, A&A, 346, 785
Slavin, J. D. & Frisch, P. C. 2002, ApJ, 565, 364
Snowden, S. L., Egger, R., Finkbeiner, D. P., Freyberg, M. J., & Plucinsky, P. P. 1998, ApJ, 493, 715
Sofia, U. J., & Jenkins, E. B. 1998, ApJ, 499, 951
Sonneborn, G., Tripp, T. M., Ferlet, R., Jenkins, E. B., Sofia, U. J., Vidal-Madjar, A., & Woźniak, P. ;. R. 2000, ApJ, 545, 277
Sonneborn, G. et al. 2002, ApJS, 140, 51
Spergel, D. N. et al. 2003, submitted to ApJ (astro-ph/0302209)
Steigman, G. 2003, ApJ, 586, 1120
Stompor, R. et al. 2001, ApJ, 561, L7
Tosi, M., Steigman, G., Matteucci, F., & Chiappini, C. 1998, ApJ, 498, 226
Timmes, F. X., Truran, J. W., Lauroesch, J. T., & York, D. G. 1997, ApJ, 476, 464
Vangioni-Flam, E., & Cassé, M. 1995, ApJ, 441, 471
Vangioni-Flam, E., Coc, A., & Cassé, M. 2000, A&A, 360, 15
Vidal-Madjar, A. et al. 1998, A&A, 338, 694
Vidal-Madjar, A. & Ferlet, R. 2002, ApJ, 571, L169
Webb, J. K., Carswell, R. F., Lanzetta, K. M., Ferlet, R., Lemoine, M., Vidal-Madjar, A., & Bowen, D. V. 1997, Nature, 388, 250
Wood, B. E., Linsky, J. L., Hébrard, G., Vidal-Madjar, A., Lemoine, M., Moos, H. W., Sembach, K. R., & Jenkins, E. B. 2002a, ApJS, 140, 91
Wood, B. E., Redfield, S., Linsky, J. L., & Sahu, M. S. 2002b, ApJ, 581, 1168
Wright, C. M., van Dishoeck, E. F., Cox, P., Sidher, S. D., Kessler, M. F. 1999, ApJ, 515, L29
York, D. G. & Kinahan, B. F. 1979, ApJ, 228, 127
York, D. G. 1983, ApJ, 264, 172

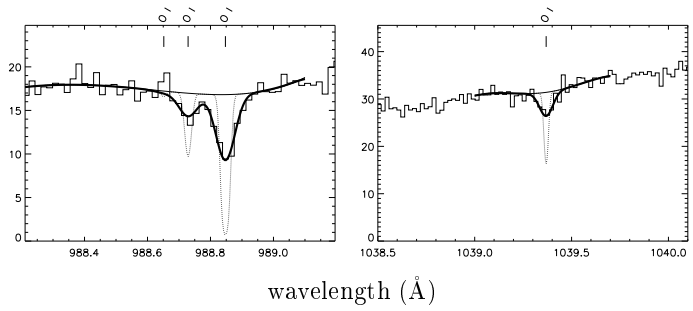

FIG. 1.— Examples of *FUSE* spectral windows fitted on the line of sight of Sirius B. The list of all the O I lines included in the fits are reported in Table 2. Histogram lines are the data, the solid lines are the fits and continua, and the dotted lines are the model profiles prior to convolution with the LSF. Y-axis is flux in 10^{-12} erg/cm^2/s/Å.

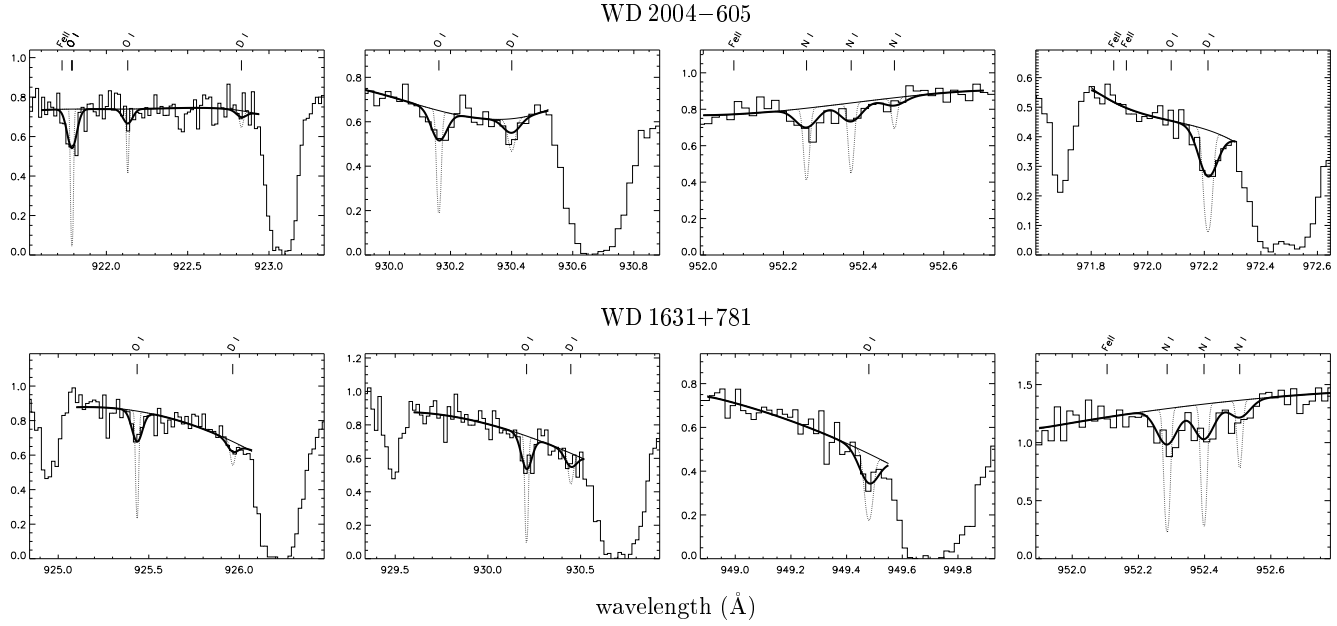

FIG. 2.— Examples of *FUSE* spectral windows fitted on the lines of sight of the DA1 white dwarfs WD 2004−605 and WD 1631+781. The list of all the D I, O I, and N I lines included in the fits are reported in Table 2. Histogram lines are the data, the solid lines are the fits and continua, and the dotted lines are the model profiles prior to convolution with the LSF. Y-axis is flux in 10^{-12} erg/cm^2/s/Å.

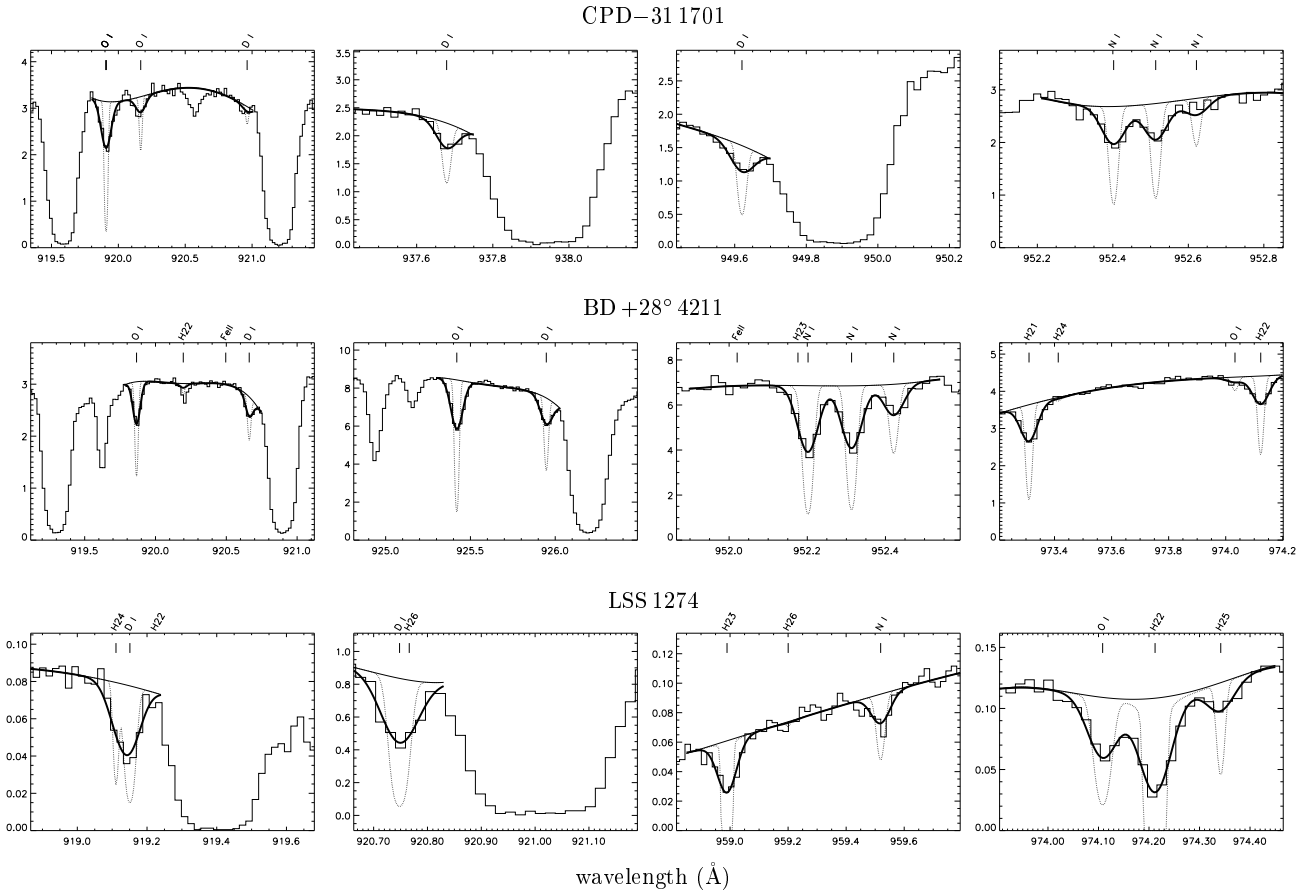

FIG. 3.— Examples of *FUSE* spectral windows fitted on the lines of sight of the sdO subdwarfs CPD−31 1701, BD +28° 4211, and LSS 1274. The list of all the D I, O I, and N I lines included in the fits are reported in Table 2. Histogram lines are the data, the solid lines are the fits and continua, and the dotted lines are the model profiles prior to convolution with the LSF. The H_2 lines of the levels $J = 2$ to $J = 6$ are noted H22 to H26. Y-axis is flux in 10^{-11} erg/cm^2/s/Å.

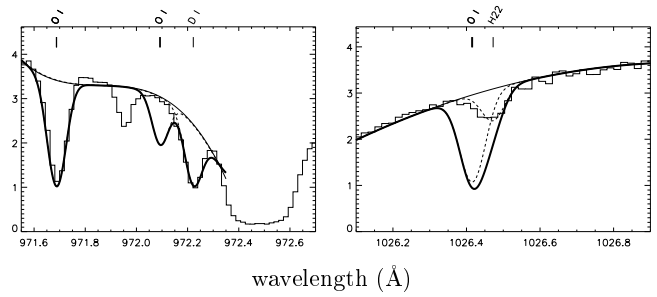

FIG. 4.— Inaccurate tabulated O I f-values. The O I lines at 972.14 Å and 1026.47 Å (wavelengths at rest) observed toward BD +28° 4211 are shown here, according to the solution found with the other lines and the f-values tabulated by Morton (1991). Histogram lines are the data, the solid lines are the computed profiles and continua, and the dashed lines are the computed profiles for each species (all convolved with the LSF). Y-axis is flux in 10^{-11} erg/cm^2/s/Å. The clear detection of other lines (O I, D I, and H_2 $J = 2$) on the two spectral windows allows wavelength shifts to be determined. The line at λ 971.95 Å is unidentified. The two tabulated f-values are too large at least by factors of 5 and 30, respectively. These two lines were not used toward any target in the present study.

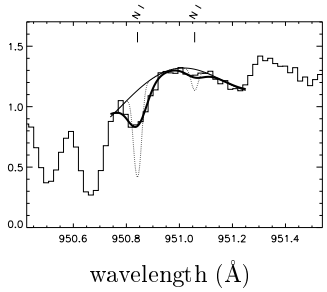

FIG. 5.— N I fit toward Feige 110. Histogram lines are the data, the solid lines are the fits and continua, and the dotted lines are the model profiles prior to convolution with the LSF. Y-axis is flux in 10^{-11} erg/cm^2/s/Å.

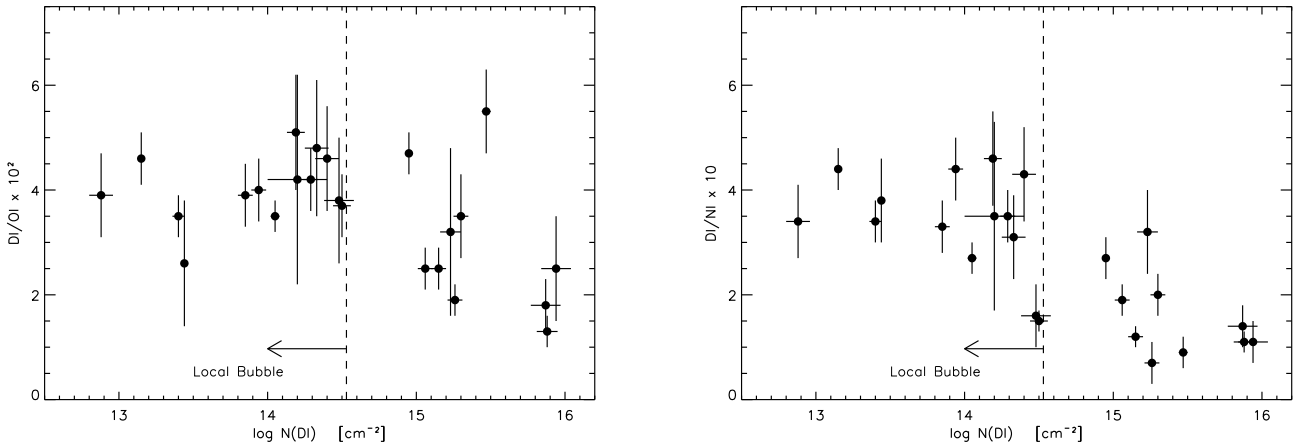

FIG. 6.— D/O and D/N measurements in the interstellar medium as a function of the D I column density. The plotted error bars are $1\,\sigma$. The dotted line indicates the limit of the Local Bubble, inside which the D/O ratio is homogeneous.

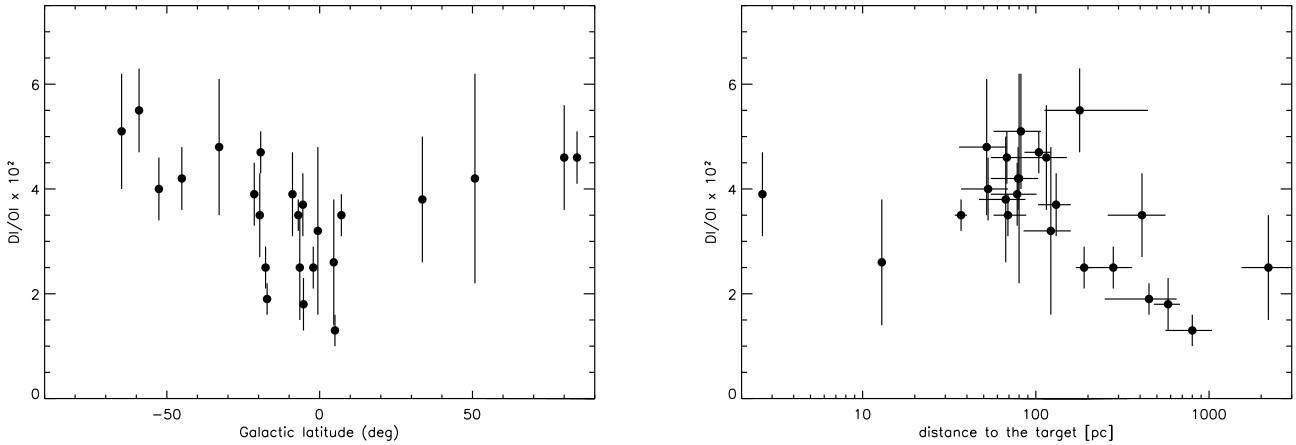

FIG. 7.— D/O measurements in the interstellar medium as a function of the Galactic latitude b and the distance of the targets. The plotted error bars are $1\,\sigma$.

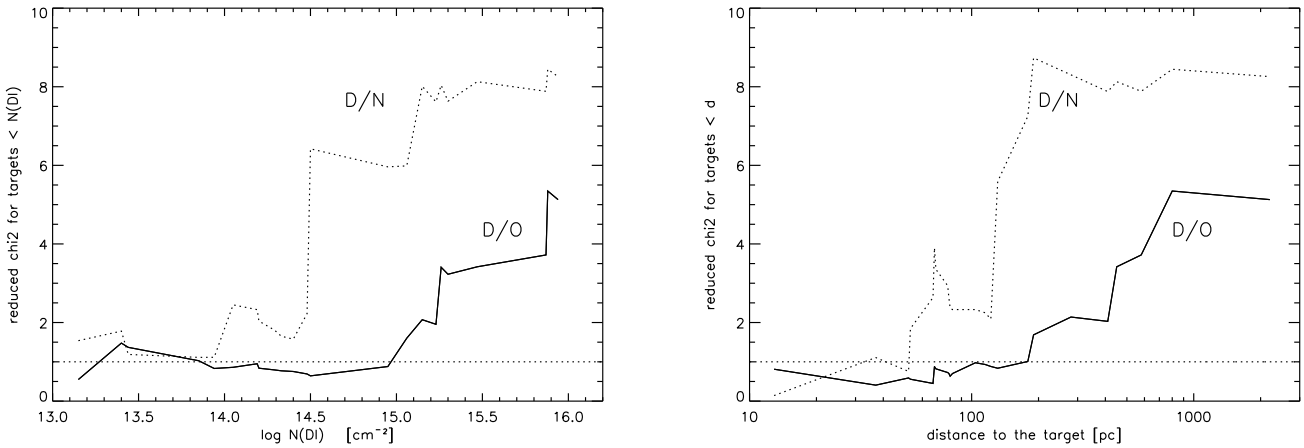

FIG. 8.— The reduced χ^2 of the D/O and D/N weighted mean as a function of the D I column density and distance upper limits assumed to define the sample used for the weighted mean calculation (see text). D/O is homogeneous for $d < 150$ pc and $\log N(\mathrm{D\ I}) < 14.5$; it shows significant spatial variations beyond these limits. D/N varies even for low $\log N(\mathrm{D\ I})$ and d values.

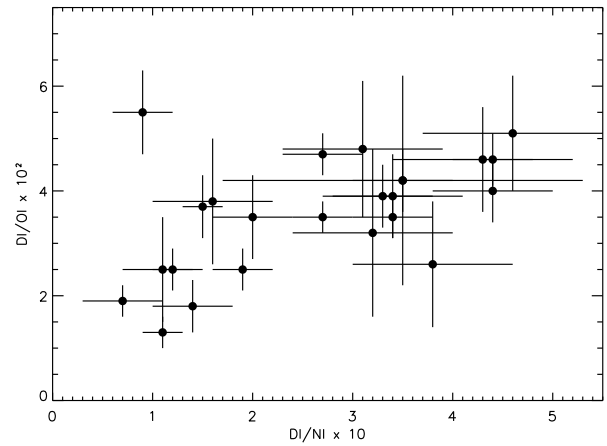

FIG. 9.— D/O measurements in the interstellar medium as a function of D/N. The plotted error bars are $1\,\sigma$.

Table 1

Log of the observations.

Target	Observation date	Observation reference	$T_{\rm obs}$ (ksec)[a]	$N_{\rm exp}^{\rm b}$	Aperture[c]	Mode[d]	CalFUSE[e]
Sirius B	2001 Nov 25	C1160102	1.6	4	MDRS	HIST	1.8.7
	2001 Nov 17	C1160103	1.3	1	MDRS	TTAG	1.8.7
	2001 Nov 25	C1160104	1.8	4	MDRS	HIST	1.8.7
		Total:	4.7	8			
WD 2004−605	2001 May 21	P2042201	10.2	12	MDRS	TTAG	2.1.6
	2001 Aug 31	P2042202	26.0	28	MDRS	TTAG	2.1.6
	2002 Apr 10	P2042203	37.6	37	MDRS	TTAG	2.1.6
		Total:	73.8	77			
WD 1631−781	2000 Jan 18	P1042901	22.1	9	MDRS	TTAG	2.0.4
	2001 Jan 31	P1042902	30.2	33	MDRS	TTAG	2.0.4
		Total:	52.3	42			
CPD−31 1701	2001 Apr 06	P2050601	7.2	12	LWRS	HIST	2.0.5
	2001 Nov 01	P2050602	9.3	19	MDRS	HIST	2.0.5
		Total:	16.5	31			
BD +28° 4211	2000 Jun 13	M1080901	2.2	4	LWRS	HIST	2.1.1
	2000 Jul 16	M1040101	16.7	36	LWRS	HIST	2.1.0
	2000 Sep 19	M1040105	7.9	17	LWRS	HIST	2.1.1
	2001 Jul 29	M1031201	3.0	5	LWRS	HIST	2.1.0
	2001 Jul 31	M1031204	2.9	5	LWRS	HIST	2.1.0
	2000 Jul 17	M1040102	24.8	52	MDRS	HIST	2.1.0
	2001 Jul 29	M1031202	2.9	6	MDRS	HIST	2.1.0
	2001 Jul 31	M1031205	2.9	6	MDRS	HIST	2.1.0
	2001 Jul 29	M1031203	2.4	5	HIRS	HIST	2.1.0
	2001 Jul 31	M1031206	2.4	5	HIRS	HIST	2.1.0
		Total:	68.1	141			
LSS 1274	2002 Mar 08	P2051702	8.0	11	MDRS	TTAG	2.1.6
	2002 Mar 11	P2051701	14.0	12	MDRS	TTAG	2.1.6
	2002 May 02	P2051703	63.0	54	MDRS	TTAG	2.1.6
		Total:	85.0	77			
Feige 110	2000 Jun 22	M1080801	6.2	8	LWRS	HIST	1.8.7
	2000 Jun 30	P1044301	21.8	48	LWRS	HIST	1.8.7
		Total:	28.0	56			

[a] Total exposure time of the observation (in 10^3 s).
[b] Number of individual exposures during the observation.
[c] LWRS, MDRS, and HIRS are, respectively, large, medium, and narrow *FUSE* slits.
[d] HIST and TTAG are respectively histogram and time-tagged photon address *FUSE* modes.
[e] Version of the pipeline used for spectral extraction.

Table 2
D I, O I, and N I lines included in the final fits.

		Sirius B	WD 2004−605	WD 1631+781	CPD−31 1701	BD +28° 4211	LSS 1274	Feige 110
λ[a]	f[b]	#[c]	#[c]	#[c]	#[c]	#[c]	#[c]	#[c]
	D I							
972.2723	2.90×10^{-2}		2	2				
949.4848	1.39×10^{-2}		2	1	4			
937.5484	7.80×10^{-3}		2	1	4	3		
930.4951	4.82×10^{-3}		2	2		3		
925.9738	3.18×10^{-3}		2	2	4	4		
922.8993	2.22×10^{-3}		2	2		3		
920.7126	1.61×10^{-3}		2	1	3	6	2	
919.1013	1.20×10^{-3}					1	2	
917.8797	9.21×10^{-4}					2	2	
916.9311	7.23×10^{-4}		1	1				
	Total:		15	12	15	22	6	–
	O I							
988.7734	4.65×10^{-2}	2						
971.738[d]	1.38×10^{-2}	1						
1039.2304	9.20×10^{-3}	3						
988.6549	8.30×10^{-3}	2						
950.8846	1.58×10^{-3}		2					
921.8570[d]	1.19×10^{-3}		2		4			
919.6580[d]	9.47×10^{-4}		2		4			
988.5778	5.53×10^{-4}	2						
930.2566	5.37×10^{-4}		2	2	4			
916.8150[d]	4.74×10^{-4}		1	1				
925.4460	3.50×10^{-4}		2	2	1	3		
922.2000	2.45×10^{-4}		2	2	2	1		
919.9170	1.78×10^{-4}		2	1	4	6		
974.0700	1.56×10^{-5}					4	2	
	Total:	10	15	8	19	14	2	–
	N I							
964.6256	9.43×10^{-3}		1					
954.1042	6.76×10^{-3}		2					
965.0413	4.02×10^{-3}		1					
952.3034	1.87×10^{-3}		2	2	4	3		
952.4148	1.70×10^{-3}		2	2	4	3		
952.5227	6.00×10^{-4}		2	2	4	3		
951.0791	1.29×10^{-4}					4	2	2
955.8816	5.88×10^{-5}					2	1	
955.2644	5.03×10^{-5}					3		
959.4937	4.98×10^{-5}						2	
951.2947	1.81×10^{-5}					4	2	2
955.5294	1.72×10^{-5}						1	
	Total:		10	6	12	22	8	4

[a] Wavelength in vacuum at rest (in Å).
[b] Oscillator strength.
[c] Number of independent lines included in the fit (observed on different channels and through different slits, using all the observations presented in Table 1).
[d] Triplet structure used (see Morton 1991; 2003)

Table 3

D I, O I, and N I interstellar column densities measured toward 24 lines of sight.

Target	Sp.	l (°)	b (°)	d (pc) [a]	log N(D I) [b]	log N(N I) [b]	log N(O I) [b]	D/N $\times 10$	D/O $\times 10^2$	Ref. [c]
Sirius B	DA2	227.2	−8.9	2.64 ± 0.01 [h]	12.88 ± 0.08	13.35 ± 0.03	14.29 ± 0.05	3.4 ± 0.7	3.9 ± 0.8	1,2
HZ 43 A	DA1	54.1	+84.2	68 ± 13 [p]	13.15 ± 0.02	13.51 ± 0.03	14.49 ± 0.04	4.4 ± 0.4	4.6 ± 0.5	3
G191−B2B	DA1	155.9	+7.1	69^{+19}_{-12} [h]	13.40 ± 0.04	13.87 ± 0.04	14.86 ± 0.04	3.4 ± 0.4	3.5 ± 0.4	4
Capella	G8III+	162.6	+4.6	12.9 ± 0.2 [h]	13.44 ± 0.01	13.86 ± 0.09	15.02 ± 0.16	3.8 ± 0.8	2.6 ± 1.2	5
WD 0621−376	DA1	245.4	−21.4	78 [p]	13.85 ± 0.05	14.34 ± 0.05	15.26 ± 0.04	3.3 ± 0.5	3.9 ± 0.6	6
WD 2211−495	DA1	345.8	−52.6	53 [p]	13.94 ± 0.05	14.30 ± 0.03	15.34 ± 0.04	4.4 ± 0.6	4.0 ± 0.6	7
WD 1634−573	DO	329.9	−7.0	37 ± 3 [h]	14.05 ± 0.03	14.62 ± 0.04	15.51 ± 0.03	2.7 ± 0.3	3.5 ± 0.3	8
WD 2331−475	DA1	334.8	−64.8	82 [p]	14.19 ± 0.06	14.53 ± 0.05	15.48 ± 0.06	4.6 ± 0.9	5.1 ± 1.1	9
α Vir	B1III-IV	316.1	+50.8	80 ± 6 [h]	14.20 ± 0.20	14.66 ± 0.05	15.58 ± 0.10	3.5 ± 1.8	4.2 ± 2.0	10
GD 246	DA1	87.2	−45.1	79 [p]	14.29 ± 0.05	14.75 ± 0.03	15.67 ± 0.04	3.5 ± 0.5	4.2 ± 0.6	9
WD 2004−605	DA1	336.6	−32.9	52 [p]	14.33 ± 0.08	14.84 ± 0.08	15.65 ± 0.08	3.1 ± 0.8	4.8 ± 1.3	1
HZ 21	DO2	175.0	+80.0	115[p]	14.40 ± 0.08	14.77 ± 0.04	15.74 ± 0.05	4.3 ± 0.9	4.6 ± 1.0	9
WD 1631+781	DA1	111.3	+33.6	67 [p]	14.48 ± 0.10	15.28 ± 0.10	15.90 ± 0.09	1.6 ± 0.6	3.8 ± 1.2	1
CPD−31 1701	sdO	246.5	−5.5	131 ± 28 [h]	14.50 ± 0.06	15.33 ± 0.04	15.93 ± 0.04	1.5 ± 0.2	3.7 ± 0.6	1
BD +28° 4211	sdO	81.9	−19.3	104 ± 18 [h]	14.95 ± 0.02	15.52 ± 0.05	16.28 ± 0.03	2.7 ± 0.4	4.7 ± 0.4	1
δ Ori A	O9.5II	203.9	−17.7	280 ± 80 [h]	15.06 ± 0.05	15.79 ± 0.04	16.67 ± 0.05	1.9 ± 0.3	2.5 ± 0.4	11,12
γ Cas	B0IVe	123.6	−2.1	190 ± 20 [h]	15.15 ± 0.05	16.06 ± 0.04	16.76 ± 0.04	1.2 ± 0.2	2.5 ± 0.4	12,13,14
Lan 23	DA	107.6	−0.6	122 [p]	15.23 ± 0.07	15.73 ± 0.07	16.72 ± 0.17	3.2 ± 0.8	3.2 ± 1.6	9
ϵ Ori	B0Ia	205.2	−17.2	450 ± 200 [h]	15.26 ± 0.05	16.45 ± 0.20	16.98 ± 0.05	0.7 ± 0.4	1.9 ± 0.3	12,15,16
ι Ori	O9III	209.5	−19.6	410 ± 150 [h]	15.30 ± 0.05	15.99 ± 0.07	16.76 ± 0.09	2.0 ± 0.4	3.5 ± 0.8	12,14,15
Feige 110	sdOB	74.1	−59.1	179^{+265}_{-67} [h]	15.47 ± 0.03	16.51 ± 0.10	16.73 ± 0.05	0.9 ± 0.3	5.5 ± 0.8	1,17
LSS 1274	sdO	277.0	−5.3	580 ± 100 [p]	15.87 ± 0.10	16.73 ± 0.05	17.62 ± 0.08	1.4 ± 0.4	1.8 ± 0.5	1
HD 195965	B0V	85.7	+5.0	800 [p]	15.88 ± 0.07	16.85 ± 0.03	17.77 ± 0.03	1.1 ± 0.2	1.3 ± 0.3	18
HD 191877	B1Ib	61.6	−6.5	2200[p]	15.94 ± 0.10	16.88 ± 0.05	17.54 ± 0.10	1.1 ± 0.4	2.5 ± 1.0	18

[a] Distances are photometric (D [p]; see references) or from Hipparcos parallax (D [h]; Perryman et al. 1997).

[b] Column densities N (in cm^{-2}); $1\,\sigma$ error bars.

[c] References for column density measurements. – (1) This work; (2) Hébrard et al. (1999); (3) Kruk et al. (2002); (4) Lemoine et al. (2002); (5) Wood et al. (2002b); (6) Lehner et al. (2002); (7) Hébrard et al. (2002); (8) Wood et al. (2002a); (9) Oliveira et al. (2003); (10) York & Kinahan (1979); (11) Jenkins et al. (1999); (12) Meyer et al. (1998) & Meyer (2001); (13) Ferlet et al. (1980); (14) Meyer et al. (1997); (15) Laurent et al. (1979); (16) Hibbert et al. (1985); (17) Friedman et al. (2002); (18) Hoopes et al. (2003)

Table 4

Deuterium abundances.

D/O in the Local Bubble	3.84 ± 0.16	$\times 10^{-2}$
D/O total in the Local Bubble (*i.e.* corrected for oxygen depletion)	~ 2.7	$\times 10^{-2}$
D/O total expected in the local interstellar medium (LISM) from chemical evolution models	$2.5 - 4$	$\times 10^{-2}$
D/O at greater distances (*i.e.* beyond the LISM)	1.50 ± 0.25	$\times 10^{-2}$
D/O in QSO absorption lines	$20 - 3000$	$\times 10^{-2}$
D/H in the Local Bubble from previous direct measurements of N(D I) and N(H I)	1.5 ± 0.1	$\times 10^{-5}$
D/H in the Local Bubble from D/O and O/H measurements	1.32 ± 0.08	$\times 10^{-5}$
D/H at greater distances (*i.e.* beyond the LISM) from D/O and O/H	0.52 ± 0.09	$\times 10^{-5}$
D/H at greater distances (*i.e.* beyond the LISM) from D/N and N/H	0.86 ± 0.13	$\times 10^{-5}$
D/H in proto-solar material (Solar wind, Jupiter, Saturn)	$2 - 3$	$\times 10^{-5}$
D/H in primordial material (QSO absorption lines and CMB)	$2.5 - 3$	$\times 10^{-5}$